

The study of glass transition temperature in Sb–V₂O₅–TeO₂ glasses at different heating rates

D Souri*

Department of Physics, Faculty of Science, Malayer University, Malayer, Iran

Received: 19 January 2015 / Accepted: 22 April 2015 / Published online: 5 June 2015

Abstract: The glass transition of $x\text{Sb}-(60-x)\text{V}_2\text{O}_5-40\text{TeO}_2$ glasses with $0 < x < 15$ (in mol%) at different heating rates ($\varphi = 3-12$ K/min) has been studied using differential scanning calorimetry. The glass transition temperature (T_g) and crystallization temperature (T_{cr}) of these glasses have been determined. The effects of the heating rate and the Sb content on T_g have been discussed. It has been observed that the transition region shifts to higher temperatures when the measuring time is reduced. The compositional dependence of T_g has been determined and so an empirical equation has been deduced relating the glass transition temperature with the Sb concentration. Also, the value of glass-forming tendency has been studied for the present glasses.

Keywords: Amorphous materials; Differential scanning calorimetry; Phase transitions; Specific heat; Glasses

PACS No.: 81.05.Gc

1. Introduction

The study of the physical and structural properties of oxide glasses is continuing to attract the attention of many researchers [1–25]. In the case of many tellurite glasses, their electrical, thermal, mechanical, optical, spectral and structural properties have been extensively investigated [1–8]. TeO₂-based glasses have attracted more attention not only because of their numerous technical applications, but also because of their high glass-forming ability, wide transmission window, suitable glass stability, high refractive index, high nonlinear optical properties, low and accessible melting point and also no hygroscopic property (suitable ambient durability) which limits the application of phosphate glasses [1–14, 26–31].

The study in thermal and structural features of glasses by differential scanning calorimetry (DSC) investigation is a suitable way to understand the behavior of glasses as a function of composition [26]. Investigation of the role of changing in glass composition on the thermal properties, the concentration of non-bridging oxygen, rigidity and packing of the structure of glass can help us to reach the

optimized composition satisfying high thermal stability against thermal shocks for technological applications.

The nature of the glass transition is a fundamental issue in the solid-state physics [27, 32]. Although the thermal properties of crystalline solids are now understood, this is not the case for amorphous materials and more works are needed to overcome this vacuum. The DSC technique is widely used to investigate the thermal properties and glass transformation in glassy materials. The kinetics of the glass transition, as studied by the DSC method, is important in investigating the nature of the glass transformation process [26, 31]. The glass transition temperature, T_g , can be accurately determined by DSC measurements. Moreover, the kinetic aspect of the glass transition is evident from the strong dependence of T_g on the heating rate [27, 31]. It has been observed that the transition region shifts to higher temperatures if the measuring time is reduced (or, conversely, if the applied heating rate is increased) [33, 34].

Some works have been published on the calorimetric features of tellurium-based glasses and ternary glasses TeO₂–V₂O₅–A_mO_n (A_mO_n is another oxide) [21–25, 35]. Mori et al. [10] have investigated the electrical properties of TeO₂–V₂O₅ samples, but there is no report on their calorimetric and glass transition temperature. The present work reports the calorimetric features of Sb–V₂O₅–TeO₂ glasses to investigate: (a) the heating rate dependence

*Corresponding author, E-mail: d.souri@gmail.com; d.souri@malayeru.ac.ir

of the glass transition temperature, (b) the effect of Sb content on the glass transition and (c) the glass-forming tendency of the samples.

2. Experimental details

The tri-component $x\text{Sb}-(60-x)\text{V}_2\text{O}_5-40\text{TeO}_2$ glasses with $0 \leq x \leq 15$ (in mol%), hereafter termed as S_x , were prepared by melting the V_2O_5 , TeO_2 and Sb in porcelain crucibles [32]. This compositional range was chosen primarily for the reason that the melts for these compositions were relatively easy to form glass. The melts for the compositions containing either $x > 15$ crystallized rapidly during quenching [36]. During the melting, the liquids were stirred every 5 min to prevent the separation of the three components. The corresponding melting temperatures were in the range of 680–730 °C. The melt was poured on to a polished steel block and immediately pressed by another polished steel block at room temperature. The obtained glasses were characterized by X-ray diffraction (XRD) studies using a diffractometer (Unisantix-XMD300, $\text{CuK}\alpha$, India). The density (ρ) of each sample was determined by the Archimedes's method using para-xylene as immersion liquid. Also, the glass transition temperature (T_g) of these samples was obtained using differential scanning calorimetry (NETZSCH DSC 200 F3, Germany) under dynamic N_2 gas atmosphere (at a constant rate of $30 \text{ cm}^3/\text{min}$) at the heating rates (φ) of 3, 6, 9 and 12 K/min. For each DSC measurement, the sample was first heated at an arbitrary heating rate (normally 20 K/min) to a temperature that is 20–30 K higher than its glass transition temperature (T_g) and held there for 5 min to erase the previous thermal history (during cooling the melt) of the glass [37]. Thus, to obtain the samples with the same initial thermal conditions and also to obtain thermal data with more precise, we used the mentioned isothermal process. After the isothermal hold, the sample was cooled at the same rate through the glass transition region to a temperature ($\sim 100 \text{ }^\circ\text{C}$) well below T_g and then reheated at a rate (φ) of 3, 6, 9 and 12 K/min to record the DSC curves [37].

3. Results and discussion

Figure 1 shows the XRD patterns of S_x samples, confirming their amorphous nature. XRD peaks for S12 are probably related to the microcrystalline phase of Sb–V in the amorphous matrix. Also, previous study [36] has reported crystalline peaks for $x = 12$ composite. The observed crystalline peaks correspond to vanadium–antimony (SbVO) phase for (110) and (101) planes.

The representative DSC plots for the sample S0 at different heating rates are shown in Fig. 2. For other samples,

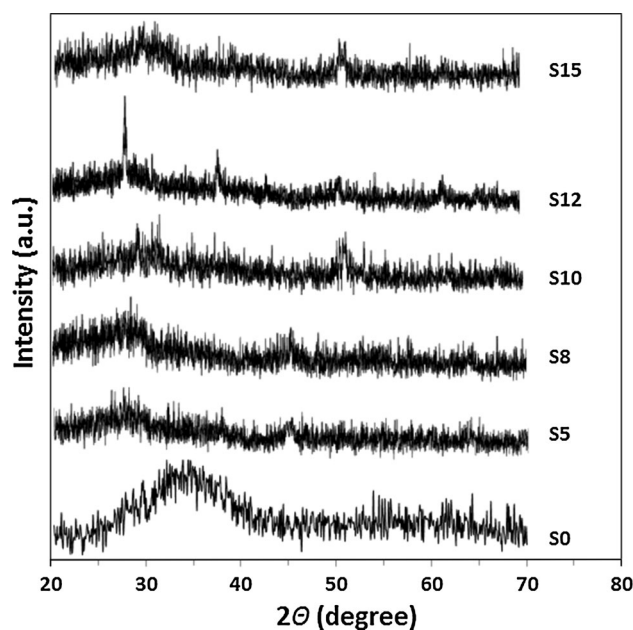


Fig. 1 XRD patterns of S_x glasses

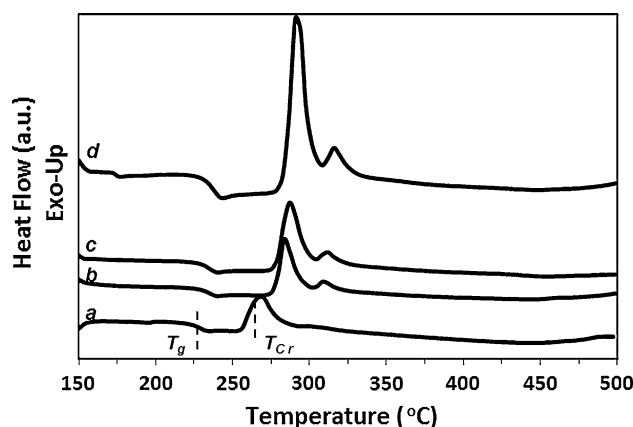


Fig. 2 DSC curves for S0 sample at different heating rates: a $\varphi = 3 \text{ K/min}$, b $\varphi = 6 \text{ K/min}$, c $\varphi = 9 \text{ K/min}$ and d $\varphi = 13 \text{ K/min}$

the obtained calorimetric data are listed in Table 1. In the absence of thermal events, the position of the baseline in such a plot is proportional to the specific heat of the sample. The presence of an endothermic peak, superimposed on the baseline, indicates the occurrence of a heat-absorbing event such as glass transition or melting. On the other hand, an exothermic peak occurs as a result of some sort of heat-releasing event such as crystallization [38]. The glass transition temperature T_g , as defined by the endothermic change in the DSC trace indicates a large change of viscosity, marking a transformation from amorphous solid phase to supercooled liquid state. As the output of the DSC during heating is proportional to the heat capacity, it is a straightforward and convenient method of

Table 1 Values of glass transition temperature (T_g), crystallization temperature (T_{cr}), glass density (ρ), glass-forming tendency (K_{gl}), and the constants A and n in Eq. (1) at the used different heating rates (φ) for S_x glasses

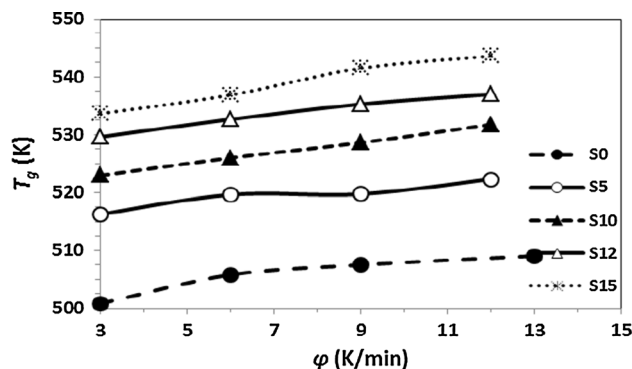
Nominal composition	φ (K/min)	T_g (°C)	T_{cr} (°C)	T_m (°C)	ρ (g cm ⁻³)	K_{gl}	$n \times 10^{-3}$	A (K)
S0	3	227.70	267.16	680	3.710	0.13	8.7	501.05
	6	232.68	283.20					
	9	234.40	286.80					
	13	235.96	290.64					
S5	3	243.30	312.22	700	3.759	0.21	8.7	501.05
	6	246.67	325.86					
	9	246.77	325.02					
	12	249.33	331.89					
S10	3	249.98	340.39	710	3.888	0.29	8.7	501.05
	6	253.01	356.52					
	9	255.65	375.08					
	12	258.78	389.71					
S12	3	256.64	411.69	720	4.031	0.65	8.7	501.05
	6	259.69	440.86					
	9	262.32	453.57					
	12	264.03	–					
S15	3	260.69	377.36	730	4.144	0.43	8.7	501.05
	6	263.91	403.65					
	9	268.54	414.99					
	12	270.65	433.04					

detecting the glass transition and investigating its kinetics. For example, the heating rate dependence of T_g can be used to determine the activation energy of the transition from glassy to liquid state [33, 39–41].

In this work, the middle point of the endothermic trace has been used to define T_g . Other definitions for T_g have been used by different workers. For instance, Abu-Sehly et al. [40] and Moynihan et al. [33] have used different definitions of T_g that include the extrapolated onset, the inflection point and the maximum point of the endothermic trace. The exothermic peak temperature T_{cr} is used to identify the crystallization process. Both T_{cr} and T_g shift to higher temperatures with increasing heating rate. The heating rate dependence of T_g is clearly seen in Figs. 2 and 3 and also Table 1. The kinetic aspect of the glass transition is evident from the pronounced shift in T_g . It is worth noting that an order of magnitude increase in φ causes a shift in T_g of about 3 K [42].

The general features of DSC thermograms for S0 glass indicate a relatively wide range between the glass transition and the crystallization temperatures, as shown in Fig. 2. These thermograms indicate that the glass transition temperature varies with the rate of heating. It increases with increase in heating rate.

The obtained values for the glass transition temperature T_g at different heating rates φ for the other compositions

**Fig. 3** Plot of glass transition temperature (T_g) versus heating rate (φ), for S_x glasses

also show similar behavior. For each composition, the variation of T_g with φ shows a nonlinear dependence as shown in Fig. 3.

Figure 3 indicates a more steep variation of T_g at a lower rate of heating. In other words, for the investigated system, the glass transition temperature is more effective at a lower heating rate. This means that the dependence of T_g on φ is more pronounced at the lower heating rate. On the other hand, the DSC data reported in Table 1 show that in all heating rates, the glass transition temperature increases with increasing antimony concentration. This variation is

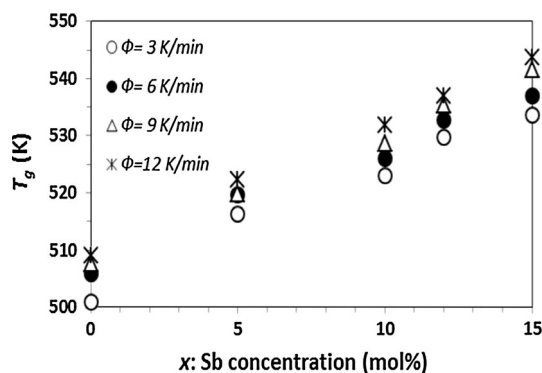


Fig. 4 Variation of T_g with the antimony concentration (x) for S_x glasses, at different heating rates (ϕ)

shown in Fig. 4, where T_g increases with increasing x or with decreasing V-content for each heating rate. Furthermore, using the results presented in Fig. 4, T_g data show that the glass transition temperature is sensitive to the Sb content. An increase in T_g can be interpreted as an increase in the thermal stability of the glass. The thermal stability of the glass is a result of the glass structure. In other words, in this work, the change in T_g indicates a change related to the manner in which V_2O_5 and Sb get arranged in the glass. The thermally stable glasses have close-packed structure, while the unstable glasses have loose-packed structure [43]. Thus, the addition of Sb increases the stability of the glass and the rigidity of the network, which is in agreement with the data of the glass density (a criterion of packing) reported in Table 1. Also, a useful parameter can be used for investigating the stability of these glasses. This parameter is thermal stability $T_S = T_{cr} - T_g$ [44]. The values of T_S have been reported in our previous work for the present samples [44], which indicate the highest thermal stability for S12. Results of thermal stability parameter are in agreement with the data of glass-forming tendency [44]. In brief, the higher thermal stability leads to the close-packed structure [44]. As discussed earlier, crystalline peaks in the XRD pattern for S12 are attributed to microcrystalline phases embedded in amorphous matrix.

It has been suggested that the glass transition temperature increases if the average coordination number increases [37, 40]. This may be due to the decrease in the number of V–V bonds and the increase in the V–Sb bonds as a result of increase in the Sb concentration (x). In other words, the cross-linking provided by Sb atoms increases for the present samples, which in turn affects the structure in a manner to increase T_g . By plotting $\ln(T_g)$ versus $x^{0.73}$, we find straight lines with different slopes, as shown in Fig. 5. In better word, to obtain the linear relation between the glass transition temperature and Sb content, the mathematical function fitting has been done by using common software. It has been found that the slope n of the straight lines depends on the heating rate ϕ , that it has a positive

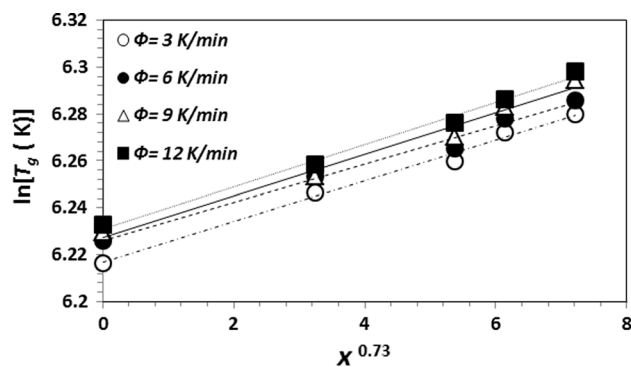


Fig. 5 Plot of $\ln T_g$ versus $x^{0.73}$ at different heating rate ϕ , for S_x glasses

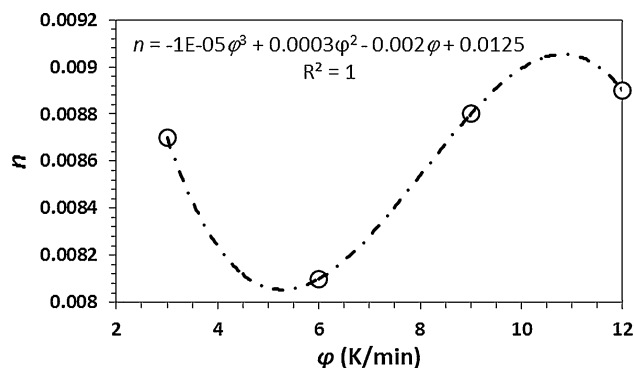


Fig. 6 Dependence of n on the heating rate, for S_x glasses

value and that it increases with increasing ϕ , except for S5. This means that the rate of variation of T_g with the antimony content x is larger for the lower heating rate. The dependence of n on the heating rate ϕ is shown in Fig. 6. It can be concluded that the relation between T_g and x within the investigated ranges obeys an empirical equation of the Arrhenius form as follows:

$$T_g = A \exp(n x^{0.73}) \quad (1)$$

where T_g is the glass transition temperature (in K), which can be calculated at any heating rate and for any antimony content within the measured range, A (in K unit) is a constant depending on ϕ and its value has been obtained by extrapolation of the linear relation in Fig. 5 to $x^{0.73} = 0$ (see also Table 1), n [in (mol%)^{-0.73}] is a constant depending on ϕ (see Table 1) and x is the antimony content. It should be mentioned that the slope n of the straight lines of $\ln(T_g) - x^{0.73}$ plots decreases for $3 \leq \phi \leq 6$ and increases for $6 \leq \phi \leq 12$. Thus, the rate of variation of T_g with the Sb content x is larger for the lower heating rate region $3 \leq \phi \leq 6$. The values of n and A can be derived at any desired heating rate within the measured range from Figs. 6 and 7, respectively. In Figs. 6 and 7, the variation of n and A can be estimated by using the equations

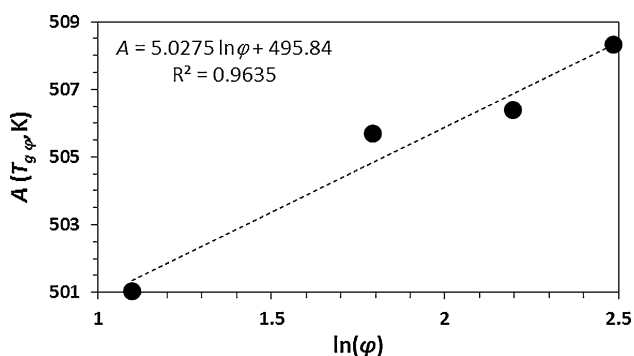


Fig. 7 Heating rate dependence of the constant A, for S_x glasses

$n = \alpha' \varphi^3 + \beta' \varphi^2 + \gamma' \varphi + \alpha''$ and $A = \alpha \ln \varphi + \beta$, respectively (as shown in the inset of these figures), where α' , β' , γ' , α'' , α and β are constants, which are illustrated in Figs. 6 and 7.

The glass-forming tendency parameter [45] ($K_{gl} = [T_{cr} - T_g]/[T_m - T_{cr}]$) has been calculated for these glasses. The value of K_{gl} varies from 0.13 to 0.65 and has the highest value for S12, as can be seen from Table 1.

4. Conclusions

The dependence heating rate on the glass transition temperature in $x\text{Sb}-(60-x)\text{V}_2\text{O}_5-40\text{TeO}_2$ glasses has been carried out using DSC technique. The increase at the glass transition temperature with antimony concentration in the investigated system obeys an equation of the Arrhenius form. The increase of T_g with increasing Sb content may be due to an increase in the number of Sb-V bonds as a result of the increasing antimony oxide content. T_g increases with increasing heating rate. The compositional dependence of T_g has been identified for the present samples, which obeys the formula $T_g = A \exp(n \ln \varphi^{0.73})$. The values of A and n are within the range of 501.05–508.31 K and 8.1–8.9, respectively. Glass-forming tendency parameter K_{gl} varies from 0.13 to 0.65 and has the highest value for S12.

References

[1] R N Hampton, W Hong, G A Saunders and R A El-Mallawany *Phys. Chem. Glasses* **29** 100 (1988)
 [2] R El-Mallawany *J. Mater. Res.* **5** 2218 (1990)
 [3] R El-Mallawany and I A Ahmed *J. Mater. Sci.* **43** 5131 (2008)
 [4] R El-Mallawany *J. Mater. Res.* **7** 224 (1992)
 [5] M M Elkholy and R El-Mallawany *Mater. Chem. Phys.* **40** 163 (1995)
 [6] M M El-Zaidia, A A Ammar and R A El-Mallawany *Phys. Status Solidi (a)* **91** 637 (1985)
 [7] H Moawad, H Jain, R El-Mallawany, T Ramadan and M El-Sharbiny *J. Am. Ceram. Soc.* **85** 2655 (2002)

[8] R El-Mallawany and A A El-Moneim *Phys. Status Solidi (a)* **166** 829 (1985)
 [9] J E Stanworth *J. Soc. Glass Technol.* **36** 217 (1952)
 [10] H Mori, H Matsuno and H Sakata *J. Non-Cryst. Solids* **276** 178 (2000)
 [11] D Souri and K Shomalian *J. Non-Cryst. Solids* **355** 1597 (2009)
 [12] D Souri and S A Salehizadeh *J. Mater. Sci.* **44** 5800 (2009)
 [13] D Souri *J. Phys. D* **41** 105102 (2008)
 [14] D Souri and M Elahi *Phys. Scr.* **75.2** 219 (2007)
 [15] D Souri *J. Non-Cryst. Solids* **356** 2181 (2010)
 [16] A Ghosh and B K Chaudhuri *J. Mater. Sci.* **22** 2369 (1987)
 [17] M Pal, K Hirota, Y Tsujigami and H Sakata *J. Phys. D* **121** 459 (2001)
 [18] A Ghosh *J. Appl. Phys.* **65** 227 (1989)
 [19] G S Murugan and Y Ohishi *J. Non-Cryst. Solids* **341** 86 (2004)
 [20] S Jayaseelan, P Muralidharan, M Venkateswarlu and N Satyanarayana *Mater. Sci. Eng. B* **118** 136 (2005)
 [21] R El-Mallawany, A Abousehly and E Yousef *J. Mater. Sci. Lett.* **19** 409 (2000)
 [22] A El-Adawy and R El-Mallawany *J. Mater. Sci. Lett.* **15** 2065 (1996)
 [23] A Abdel-Kader, R El-Mallawany and M M Elkholy *J. Appl. Phys.* **73** 71 (1993)
 [24] S Sen and A Ghosh *J. Mater. Res.* **15** 995 (2000)
 [25] M A Sidkey, R El-Mallawany, A Abousehly and Y B Saddeek *Glass Sci. Technol.: Glastechnische Berichte* **75** 87 (2002)
 [26] G Turkey and M Dawy *Mater. Chem. Phys.* **77** 48 (2002)
 [27] G W Scherer *Relaxation in Glasses and Composites* (New York: Wiley) (1986)
 [28] E Gerlach *The Physics of Selenium and Tellurium* (Berlin, New York: Springer) P Grosse (Ed.) (1979)
 [29] S G Bishop, U Strom and P C Taylor *Phys. Rev. Lett.* **34** 1346 (1975)
 [30] J Donohue *The Structure of the Elements* (New York: Wiley) (1974)
 [31] CT Moynihan, A J Easteal, J Wilder and J Tucker *J. Phys. Chem.* **78** 2673 (1974)
 [32] S R Elliott *Physics of Amorphous Materials*, 2nd edn. (Essex, UK: Longman Scientific and Technical) (1990)
 [33] I Avramov, G Guinev and A C M Rodrigues *J. Non-Cryst. Solids* **271** 12 (2000)
 [34] D Zhu, C S Ray, W Zhou and D E Day *J. Mater. Sci.* **39** 7351 (2004)
 [35] K Segal, Y Kuroda and H Sakata *J. Mater. Sci.* **33** 1303 (1998)
 [36] D Souri, P Azizpour and H Zaliani *J. Electron. Mater.* **43** 3672 (2014)
 [37] D Zhu, C S Ray, W Zhou and D E Day *J. Non-Cryst. Solids* **319** 247 (2003)
 [38] G W Smith, F E Pinkerton and J J Moleski *Thermochim. Acta* **342** 31 (1999)
 [39] S Vyazovkin, N Sbirrazzuoli and I Dranca *Macromol. Rapid Commun.* **25** 1708 (2004)
 [40] A Abu-Sehly, M Abu El-Oyoun and A A Elabbar *Thermochem. Acta* **472** 25 (2008)
 [41] J Rocherull'e, M Matecki and Y Delugeard *J. Non-Cryst. Solids* **238** 51 (1998)
 [42] M Lasocka *Mater. Sci.* **23** 173 (1976)
 [43] R N Sinclair, A C Wrigth, B Bachra, Y B Dimitriev, V V Dimitrov and M G Arnaudov *J. Non-Cryst. Solids* **232–234** 38 (1998)
 [44] D Souri, M Mohammadi and H Zaliani *Electron. Mater. Lett.* **10** 1103 (2014)
 [45] R El-Mallawany *J. Mater. Sci.: Mater. Electron.* **6** 1 (1995)